*Scientific paper*

# Novel Thiazolactone Derivatives: Synthesis and Quantum Chemical Study

**Behzad Khalili* and Niloofar Bakhshi Boroon**

*Department of Chemistry, Faculty of Sciences, University of Guilan, P.O. Box 41335-1914, Rasht, Iran*

** Corresponding author: E-mail: b.khalili@guilan.ac.ir*
*Tel.:+981333367262 and fax: +981333367262*

*Received: 12-03-2022*

## Abstract

In this research, 15 novel derivatives of the thiazolactone skeleton were synthesized using the Erlenmeyer–Plöchl reaction procedure. Glycine, alanine and leucine amino acids were used to make dithiocarbamate precursor by reacting amino acids with carbon disulfide and benzyl chloride. Obtained benzyl dithiocarbamate underwent thiazolactone formation in the presence of acetic anhydride and then condensed with arylglyoxals as condensing carbonyl group source. Products were characterized using their spectroscopic IR, $^{1}$H NMR, and $^{13}$C NMR data. In continuation, computational chemistry methods were used to get some information about the products such as structural characteristics, charge distribution, $^{1}$H NMR and UV-visible spectra. Results showed that the calculated chemical shifts are in good agreement with experimentally recorded ones. The B3LYP density functional method in conjunction with the 6-311++G(d,p) basis set was used for all calculations.

**Keywords**: Thiazolactone; Erlenmeyer–Plöchl reaction; Amino acids; DFT study

## 1. Introduction

Azlactones were synthesized for the first time in 1893 by Erlenmeyer and Plöchl by the condensation reaction between benzaldehyde and *N*-acetylglycine in the presence of acetic anhydride and sodium acetate in the manner that cyclization of the *N*-acetylglycine followed by the Perkin condensation yields the products that are called Erlenmeyer azlactones (Scheme 1).[1] Erlenmeyer azlactones have been used as precursors for many important biological and industrial compounds such as peptides, drugs, pesticides, herbicides, fungicides and agrochemical intermediates. Azlactones also show an inhibition activity against tyrosinase enzyme. Some of their diaryl derivatives show inhibition of cyclooxygenase-2 (COX-2), *in vivo* anti-inflammatory and excellent activities against of arthritis and hyperalgesia.[2–4]

Different sources of carbonyl functional group containing compounds are used to synthesize various Erlenmeyer products.[5–8] In addition modifications other than using different carbonyl compounds such as using other reagents than acetic anhydride such as triphenylphosphine[9] are used for the Erlenmeyer reaction. Preparation of oxazolones[10–12] using acetic anhydride and $\alpha$-($\alpha$-haloacyl)amino acids as starting materials was reported by Bergmann and Stern.[13] *N*-Chloroacetylphenylalanine with acetic anhydride were refluxed according to the Bergmann and Stern procedure to give 4-benzylidene-2-methyl-2-oxazolin-5-one (Scheme 2).

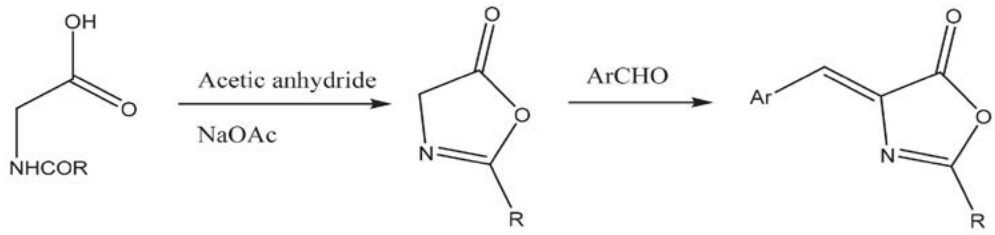


**Scheme 1.** Erlenmeyer–Plöchl reaction

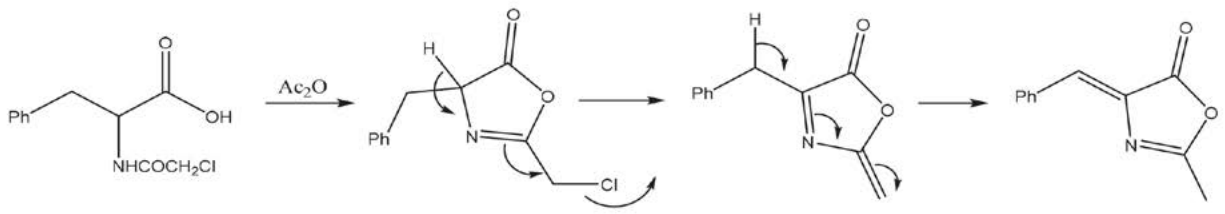

**Scheme 2.** Bergman reaction

Using amino acid-derived dithiocarbamates as precursors for the Erlenmeyer reaction is one of the recent modifications for acquiring different analogs of azlactones, as reported by Ziyaei *et al.*[14] In this protocol at first dithiocarbamates were synthesized using the reaction of the carbon disulfide, amino acids and an alkyl or benzyl halide. The product of the first step (alkyl/benzyl dithiocarbamate) undergoes azlactonization according to the Erlenmeyer procedure in the presence of acetic anhydride and sodium acetate followed by the reaction with an aromatic aldehyde to give corresponding products, which are thiazolones instead of oxazolones (Scheme 3). Oxazolones undergo various reactions to give important products with a variety of applications.

In this study we try to synthesize new derivatives of thiazolactones based on amino acid-derived dithiocarbamates. Arylglyoxals are used instead of simple aromatic aldehydes at the Perkin condensation step, therefor the products are conjugated enone derivatives of thiazolactones instead of their ethenyl derivatives. This modification leads to thiazolactones with broader reaction scope than the previous methods used before, because of the existence of two carbonyl compounds nearby the new carbon–carbon double bond is generated. The newly inserted carbonyl function lets the thiazolactone to undergo cyclization with an amine source such as ammonia and hydrazine to make new five and six membered heterocycles, this being the aim of our next study. Arylglyoxals are

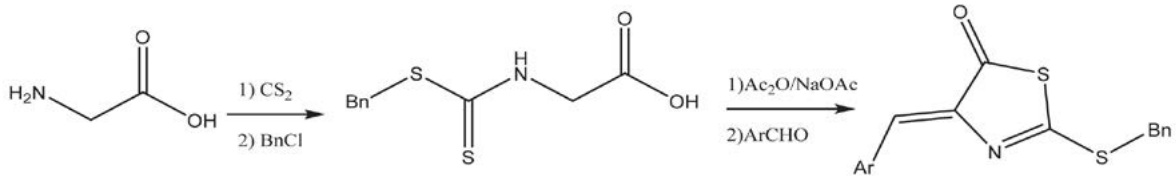

**Scheme 3.** Thiazolone synthesis

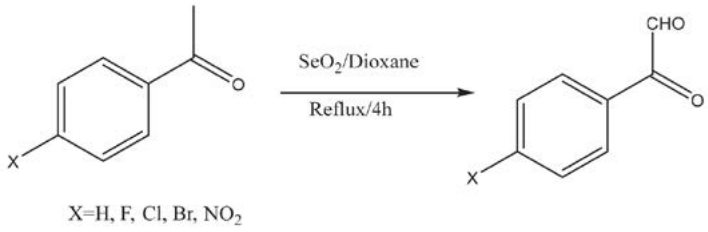

**Scheme 4.** Synthesis of arylglyoxals

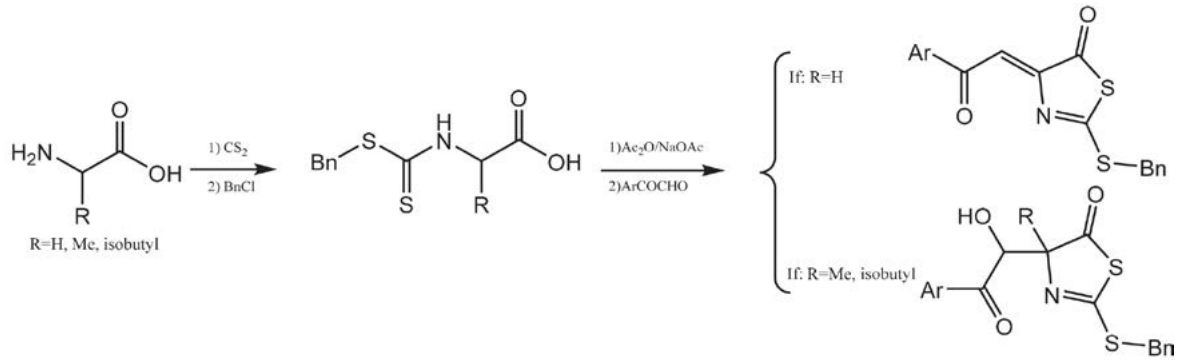

**Scheme 5.** Overall reaction studied here

oxidation products of the acetophenones in the presence of the selenium dioxide in dioxane as the solvent. They are used as very applicable precursors in heterocyclic synthetic chemistry.[15–22] The general reaction scheme for transforming acetophenones to glyoxals is shown in Scheme 4.

From the available acetophenones we made corresponding arylglyoxal derivatives and made use of them in the second step of the Erlenmeyer reaction of amino acid-based dithiocarbamates. The overall reaction is shown in Scheme 5.

## 2. Result and Discussion

In continuation of our research toward the synthesis of novel heterocyclic compounds,[16–27] herein we report an efficient synthesis of a novel class of azlactone derivatives via a one-pot reaction of amino acids, carbon disulfide, aryl or alkyl halides and arylglyoxals as outlined in Scheme 5.

Our literature survey revealed that the glyoxals have not been yet used in the Erlenmeyer reaction, therefore we used them to produce new azlactone derivatives with two carbonyl functional groups that could be promising candidates as precursors for five membered heterocycles obtained via Paal–Knorr method which makes use of 1,4-dicarbonyl compounds as the main starting material. They also can be used for the synthesis of new pyridazine derivatives if they react with hydrazine or its derivatives.

For this purpose, we investigated a one-pot reaction between arylglyoxals and the azlactone intermediates which are made during the reaction of amino acids, $CS_2$ and aryl/alkyl halides. At first, glycine was used as the amino acid source and its reaction with $CS_2$ and benzyl chloride and then phenylglyoxal in the presence of acetic anhydride and sodium acetate gave the desired products that were named as 4X-Gly where X = H, F, Cl, Br and $NO_2$ in this article. The reaction is performed under solvent-free conditions due to the simplicity and to improve the reaction rate.

Replacing glycine with alanine and also leucine as an amino acid source in this reaction gives products named as 4X-Ala and 4X-Leu where X = H, F, Cl, Br and $NO_2$, respectively. In the case of the latter two ones, elimination of the water molecule from the last product does not occur as we expected because of lacking of a hydrogen atom nearby the hydroxyl group containing carbon atom. Therefore, using alanine and leucine as amino acids gave different products than the glycine in which the hydroxyl group is present instead of a conjugated carbon-carbon double bond. Because of such differences in the product structures we may expect that the former ones incorporate substitution reactions via OH group and the latter ones incorporate an addition and also a conjugated addition reactions to make diverse derivatives with different applications. All these reveal that the described products could be very useful for discovering new organic compounds with various applications.

The reaction was carried out using the classical method in the presence of acetic anhydride and sodium acetate. Arylglyoxals including Ph, 4F-$C_6H_4$-, 4Cl-$C_6H_4$-,

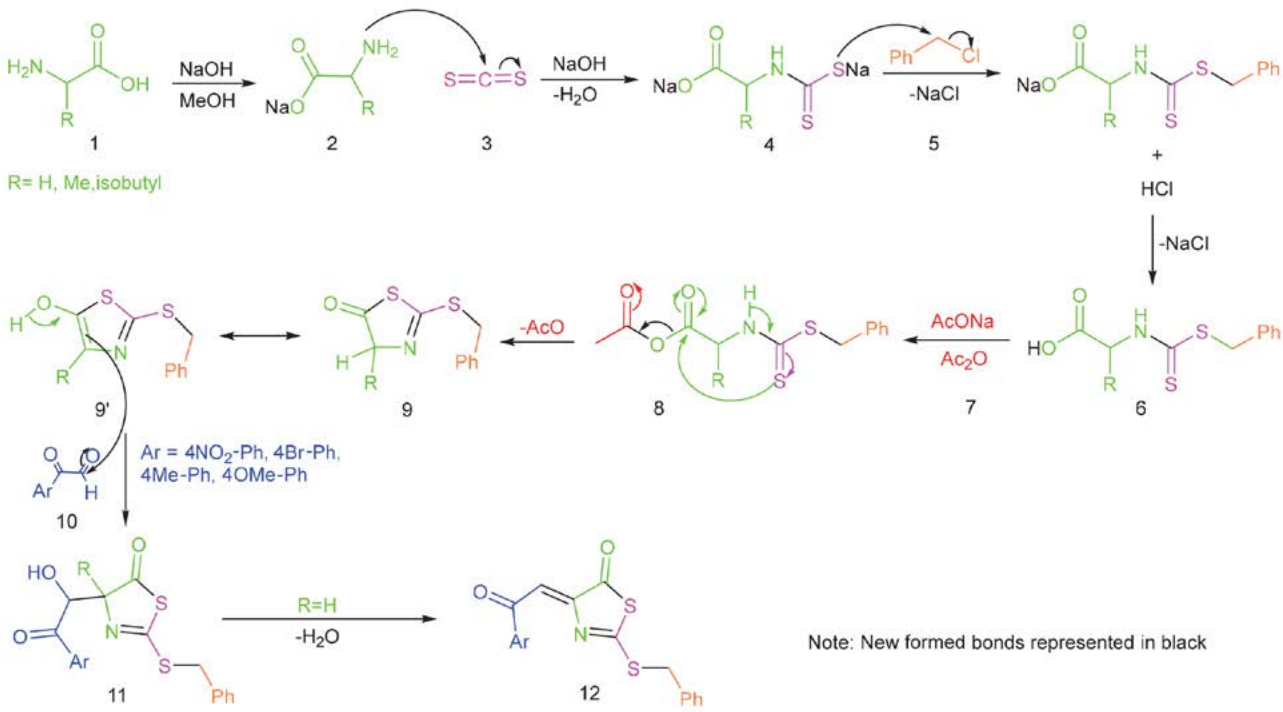


**Scheme 6.** Proposed mechanism

**Table 1**. Synthesized new thiazolactones. Optimized structure of the products are also included.

| Comp. | Optimized Structure | Intramolecular Hydrogen Bond Distance (Å) & Angle (°) | Yield (%) m.p. (°C) |
|---|---|---|---|
| 4H-Gly | 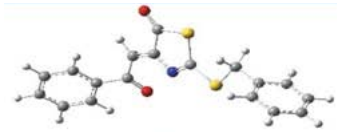 | — | 64<br>93–97 |
| 4F-Gly | 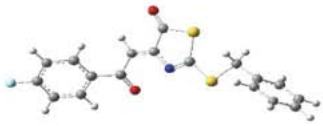 | — | 68<br>104–106 |
| 4Cl-Gly | 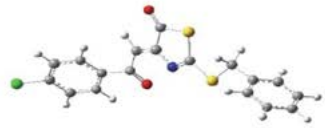 | — | 72<br>98–101 |
| 4Br-Gly |  | — | 87<br>124–125 |
| 4$NO_2$-Gly | 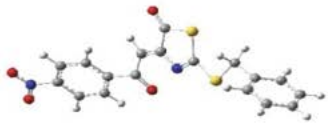 | — | 81<br>117–119 |
| 4H-Ala | 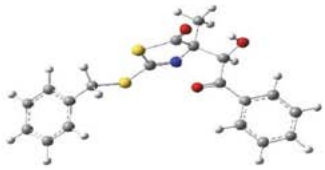 | 2.191<br>133.05 | 74<br>101–103 |
| 4F-Ala | 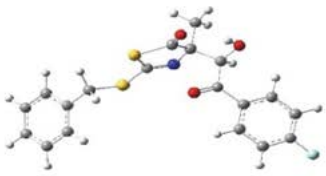 | 2.179<br>133.39 | 84<br>163–166 |
| 4Cl-Ala | 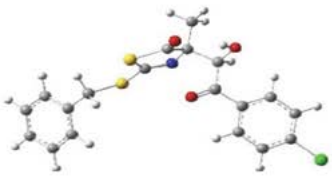 | 2.179<br>133.46 | 81<br>152–155 |
| 4Br-Ala | 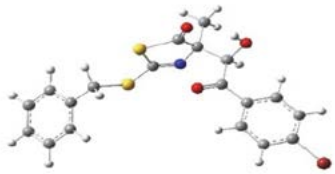 | 2.185<br>133.34 | 79<br>147–150 |
| 4$NO_2$-Ala | 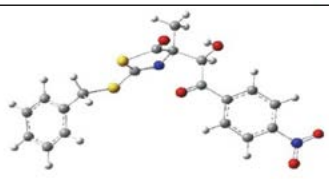 | 2.162<br>134.23 | 86<br>113–114 |

| Comp. | Optimized Structure | Intramolecular Hydrogen Bond Distance (Å) & Angle (°) | Yield (%) m.p. (°C) |
|---|---|---|---|
| 4H-Leu | 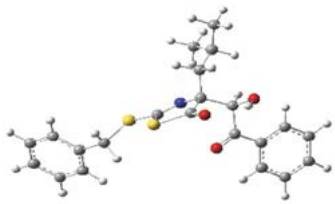 | 2.190<br>133.53 | 69<br>113–117 |
| 4F-Leu | 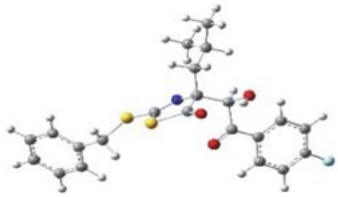 | 2.195<br>133.29 | 67<br>149–153 |
| 4Cl-Leu | 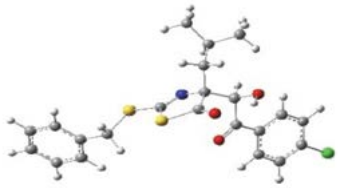 | 2.154<br>134.54 | 64<br>176–178 |
| 4Br-Leu | 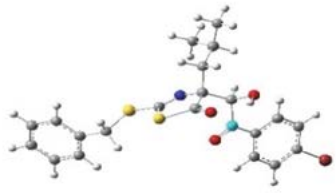 | 2.186<br>133.62 | 73<br>141–144 |
| $4NO_2$-Leu | 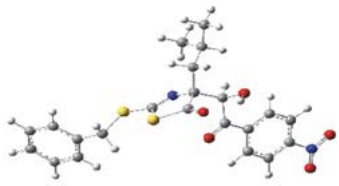 | 2.162<br>134.50 | 58<br>121–125 |

$4Br\text{-}C_6H_4$-, and $4NO_2\text{-}C_6H_4$- rings were prepared from the corresponding acetophenones and used in this reaction. Three amino acids including glycine, alanine and leucine were selected as amino acid sources and finally benzyl chloride was used as aryl halide substrate.

In all cases, the reaction proceeds through the known reaction mechanism. The only difference is that in the case of using of alanine and leucine the final step (dehydration) does not occur because of lacking of a hydrogen atom at the adjacent carbon atom to the one bearing hydroxyl group. All of the reactions are completed in almost 4 hours and led to the desired products in high yields. The results are presented in Table 1.

A proposed mechanism for this reaction is given in Scheme 6. It is proposed that at first the reaction of amino acid **1** with carbon disulfide **3** in the presence of sodium hydroxide in methanol as the solvent produced the corresponding dithiocarbamic acid anion **4** which then attacks the benzyl chloride **5** in a $S_N2$ mechanism to afford benzyl dithiocarbamic acid **6** after workup with hydrochloric acid. Benzyl dithiocarbamic acid **6** in the presence of acetic anhydride and sodium acetate undergoes intramolecular cyclization via attacking a nucleophilic sulfur atom to the most electrophilic carbon atom to produce thiazolactone **9** after eliminating one acetate anion. Thiazolactone **9** can be tautomerized to the second form of **9'** which is the enol form of the thiazolactone **9**. Then thiazolactone **9'** as a nucleophile attacks the aldehyde carbonyl group as the most electrophilic moiety of arylglyoxal **10** to produce compound **11**, which could undergo dehydration to afford compound **12** where the R group is hydrogen atom.[14,28]

# 3. Experimental

## 3. 1. General

All reagents and solvents were purchased from Merck or Fluka chemical companies and used without further purification. Melting points were measured on an Electro thermal apparatus. IR spectra were recorded on a

VERTEX 70 Bruker spectrometer. $^1$H and $^{13}$C NMR spectra of isolated products were recorded on a Bruker DRX-400 Avance (measuring frequency: $^1$H NMR 400 MHz, $^{13}$C NMR 100 MHz) in $CDCl_3$ solution. Elemental analyses were performed using a Leco Analyzer 932.

## 3. 2. Typical Procedure for the Synthesis of Dithiocarbamates

In a test tube equipped with a magnetic stir bar, amino acid (5 mmol (equals about 0.38 g of Gly, 0.45 g of Ala and 0.66 g of Leu)) and sodium hydroxide (10 mmol, 0.40 g) were dissolved in methanol (10 mL). The mixture was cooled in an ice bath (–5 °C) and then carbon disulfide (6 mmol, 0.46 g) was added and the mixture was stirred for 1 h. Then benzyl chloride (5.5 mmol, 0.70 g) was added and let the reaction mixture reach the room temperature and stirring was continued for 15 h at room temperature. Progress of the reaction was checked using TLC (ethyl acetate : *n*-hexane 3 : 1). After completion of the reaction 0.1 M aqueous HCl was added until the reaction media pH reached 5. At this point the crude product solidified. The crude product was filtered and washed twice with distilled water (20 mL). In continuation it was dried and recrystallized from ethanol to get pure product.[14] The known 6-Gly and 6-Ala dithiocarbamic acid products (in the case of using glycine and alanine as the amino acid, respectively) were verified by comparing melting points and the new 6-Leu dithiocarbamic acid product (in the case of using leucine as the amino acid) was characterized by its IR, $^1$H and $^{13}$C NMR spectra and CHN analysis (See section 3. 5).

## 3. 3. Typical Procedure for the Synthesis of Arylglyoxals

Arylglyoxals were prepared by oxidation of the acetophenone derivatives with selenium dioxide in dioxan/water solvent mixture under reflux condition according to the full detailed reported procedure.[29] The crude product could be recrystallized from boiling water to get its hydrated form.

## 3. 4. Typical Procedure for the Synthesis of Thiazolactones

In a test tube equipped with a magnetic stir bar, dithiocarbamic acid (1 mmol, (0.241 g of 6-Gly, 0.255 g of 6-Ala or 0.297 g of 6-Leu)), acetic anhydride (2.5 mmol, 0.255 g) and anhydrous sodium acetate (0.75 mmol, 0.061 g) were mixed and kept at 80 °C for 1 h with stirring. In continuing to this dark brown mixture the arylglyoxal (1.2 mmol, 0.182 g) was added. The reaction continued under the same conditions for the next 1 h. Progress of the reaction was monitored using TLC (ethyl acetate : *n*-hexane 10 : 1). Then the reaction mixture was cooled and kept in a refrigerator (2–4 °C) for 24 h. Thereafter, distilled water (15 mL) was added to the reaction mixture and stirred vigorously. The resulting solid crude product was filtered and washed first with distilled water (2 × 15 mL) and then with *n*-hexane (2 × 15 mL) to get the pure product.

## 3. 5. Characterization Data of the New Products

**((Benzylthio)carbonothioyl)leucine (6-Leu).** Yield 71%, m.p. 127–130 °C, FT-IR (KBr): *ν* ($cm^{-1}$) 3264, 3021, 2927, 1651, 1492, 695. $^1$H NMR (400 MHz, $CDCl_3$): δ (ppm) 0.91 (d, 6H, $CH_3$), 1.51 (m, 1H, CH), 1.72 (m, 2H, $CH_2$), 4.13 (s, 2H, $CH_2$), 4.17 (m, 1H, CH), 7.25–7.28 (m, 5H, ArH); $^{13}$C NMR (100 MHz, $CDCl_3$: δ (ppm) 22.7, 27.1, 36.9, 43.4, 64.3, 80.3, 128.9, 129.3, 136.4, 175.4, 196.5. Anal. calcd. for $C_{14}H_{19}NO_2S_2$: C, 56.54: H, 6.44; N, 4.71; S, 21.56. Found: C, 56.34; H, 6.74; N, 4.60; S, 21.50.

**(*Z*)-2-(Benzylthio)-4-(2-oxo-2-phenylethylidene)thiazol-5(4*H*)-one (4H-Gly).** Yield 64%, m.p. 93–97 °C, FT-IR (KBr): ν ($cm^{-1}$) 3026, 2926, 1727, 1456, 1392, 1277, 1126, 699. $^1$H NMR (400 MHz, $CDCl_3$): δ (ppm) 4.67 (s, 2H), 7.13 (s, 1H, CH), 7.46 (m, 5H, ArH), 7.85 (m, 5H, ArH); $^{13}$C NMR (100 MHz, $CDCl_3$): δ (ppm) 37.8, 49.3, 103.1, 127.6, 128.5, 128.8, 128.9, 129.0, 134.4, 136.1, 137.6, 162.8, 185.8, 193.5. Anal. calcd. For $C_{18}H_{13}NO_2S_2$: C, 63.69; H, 3.86; N, 4.13. Found: C, 63.45; H, 3.74; N, 4.26.

**(*Z*)-2-(Benzylthio)-4-(2-(4-fluorophenyl)-2-oxoethylidene)thiazol-5(4*H*)-one (4F-Gly).** Yield 68%, m.p. 104–106 °C, FT-IR (KBr): ν ($cm^{-1}$) 3078, 2957, 1696, 1601, 1510, 1443, 1230, 1126, 1029, 603. $^1$H NMR (400 MHz, $CDCl_3$): δ (ppm) 4.44 (s, 2H, $CH_2$), 6.87 (s, 1H, CH), 7.19 (m, 1H, ArH), 7.27 (m, 2H, ArH), 7.39 (m, 2H, ArH), 7.68 (d, 2H, *J* = 8.8 Hz), 7.80 (d, 2H, *J* = 8.6 Hz); $^{13}$C NMR (100 MHz, $CDCl_3$): δ (ppm) 37.7, 103.6, 115.3, 115.6, 128.7, 128.8, 128.9, 129.8, 129.9, 131.3, 131.76, 134.5, 134.9, 137.7, 162.1, 163.5, 186.5, 194.1. Anal. calcd. for $C_{18}H_{12}FNO_2S_2$: C, 60.49; H, 3.38; N, 3.92. Found: C, 60.63; H, 3.21; N, 3.64.

**(*Z*)-2-(Benzylthio)-4-(2-(4-chlorophenyl)-2-oxoethylidene)thiazol-5(4*H*)-one (4Cl-Gly).** Yield 72%, m.p. 101–98 °C, FT-IR (KBr): ν ($cm^{-1}$) 3048, 2924, 1792, 1643, 1549, 1384, 1227, 694. $^1$H NMR (400 MHz, $CDCl_3$): δ (ppm) 4.43 (s, 2H), 6.88 (s, 1H, CH), 7.51 (m, 5H, ArH), 7.72 (d, 2H, *J* = 8.4 Hz), 7.89 (d, 2H, *J* = 8.4 Hz); $^{13}$C NMR (100 MHz, $CDCl_3$): δ (ppm) 37.2, 103.6, 128.2, 128.7, 128.7, 129.5, 129.6, 129.7, 129.8, 129.9, 129.9, 134.9, 135.7, 136.7, 137.5, 162.2, 186.5, 193.5. Anal. calcd. for $C_{18}H_{12}ClNO_2S_2$: C, 57.83; H, 3.24; N, 3.75. Found: C, 58.05; H, 3.43; N, 3.52.

**(*Z*)-2-(Benzylthio)-4-(2-(4-bromophenyl)-2-oxoethylidene)thiazol-5(4*H*)-one (4Br-Gly).** Yield 78%, m.p. 124–125 °C, FT-IR (KBr): ν ($cm^{-1}$) 3035, 2924, 1722, 1621,

1440, 1383, 1268, 1070, 619. $^1$H NMR (400 MHz, $CDCl_3$): δ (ppm) 4.42 (s, 2H, $CH_2$), 6.89 (s, 1H, CH), 7.19 (m, 1H, ArH), 7.27 (m, 2H, ArH), 7.65 (m, 2H, ArH), 7.96 (d, 2H, *J* = 8.4 Hz), 7.79 (d, 2H, *J* = 8.4 Hz); $^{13}$C NMR (100 MHz, $CDCl_3$): δ (ppm) 36.9, 101.3, 124.5, 128.7, 128.7, 128.8, 129.1, 129.2, 130.3, 130.6, 132.3, 132.4, 134.9, 136.7, 137.5, 162.2, 187.3, 193.8. Anal. calcd. for $C_{18}H_{12}BrNO_2S_2$: C, 51.68; H, 2.89; N, 3.35. Found: C, 51.45; H, 3.10; N, 3.55.

**(*Z*)-2-(Benzylthio)-4-(2-(4-nitrophenyl)-2-oxoethylidene)thiazol-5(4*H*)-one (4$NO_2$-Gly).** Yield 81%, m.p. 117–119 °C, FT-IR (KBr): ν ($cm^{-1}$) 3066, 2860, 1692, 1603, 1533, 1348, 1220, 1010, 1013, 724. $^1$H NMR (400 MHz, $CDCl_3$): δ (ppm) 4.44 (s, 2H, $CH_2$), 7.18 (s, 1H, CH), 7.24 (m, 3H, ArH), 7.27 (m, 2H, ArH), 7.94 (d, 2H, *J* = 8.4 Hz), 8.10 (d, 2H, *J* = 8.4 Hz); $^{13}$C NMR (100 MHz, $CDCl_3$): δ (ppm) 37.8, 103.6, 117.3, 117.3, 128.8, 128.8, 129.8, 129.9, 134.4, 134.4, 134.8, 136.0, 137.1, 140.7, 162.1, 186.5, 193.6. Anal. calcd. for $C_{18}H_{12}N_2O_4S_2$: C, 56.24; H, 3.15; N; 7.29. Found: C, 56.51; H, 3.37; N, 6.95.

**2-(Benzylthio)-4-(1-hydroxy-2-oxo-2-phenylethyl)-4-methylthiazol-5(4*H*)-one (4H-Ala).** Yield 74%, m.p. 101–103 °C, FT-IR (KBr): ν ($cm^{-1}$) 3416, 3018, 2926, 2859, 1728, 1629, 1384, 1275, 1126, 702, 619. $^1$H NMR (400 MHz, $CDCl_3$): *δ* (ppm) 1.57 (s, 3H, $CH_3$), 4.22 (s, 2H, $CH_2$), 5.43 (d, 1H, *J* = 3.2 Hz), 7.27 (m, 5H, ArH), 7.96 (m, 5H, ArH); $^{13}$C NMR (100 MHz, $CDCl_3$): δ (ppm) 27.6, 37.8, 63.4, 79.0, 128.4, 128.5, 128.6, 128.7, 128.7, 128.9, 129.3, 129.3, 129.6, 129.6, 131.8, 134.8, 161.7, 193.8, 196.6. Anal. calcd. for $C_{19}H_{17}NO_3S_2$: C, 61.43; H, 4.61; N, 3.77. Found: C, 61.27; H, 4.46; N, 3.60.

**2-(Benzylthio)-4-(2-(4-fluorophenyl)-1-hydroxy-2-oxoethyl)-4-methylthiazol-5(4*H*)-one (4F-Ala).** Yield 84%, m.p. 163–166 °C, FT-IR (KBr): ν ($cm^{-1}$) 3457, 3064, 2982, 1698, 1578, 1388, 1221, 1114, 634. $^1$H NMR (400 MHz, $CDCl_3$): δ (ppm) 1.55 (s, 3H, $CH_3$), 4.22 (s, 2H, $CH_2$), 5.43 (s, 1H, CH), 7.24 (m, 1H, ArH), 7.25 (m, 2H, ArH), 7.27 (m, 2H, ArH), 7.44 (d, 2H, *J* = 8.4 Hz), 7.91 (d, 2H, *J* = 8.4 Hz); $^{13}$C NMR (100 MHz, $CDCl_3$): δ (ppm) 28.3, 36.1, 64.0, 76.1, 114.5, 114.6, 128.7, 128.8, 128.9, 129.4, 129.7, 131.4, 131.5, 131.7, 134.9, 162.6, 163.7, 193.6, 197.6. Anal. calcd. for $C_{19}H_{16}FNO_3S_2$: C, 58.60; H, 4.14; N, 3.60. Found: C, 58.46; H, 4.39; N, 3.75.

**2-(Benzylthio)-4-(2-(4-chlorophenyl)-1-hydroxy-2-oxoethyl)-4-methylthiazol-5(4*H*)-one (4Cl-Ala).** Yield 81%, m.p. 152–155 °C, FT-IR (KBr): ν ($cm^{-1}$) 3377, 3038, 2972, 1695, 1589, 1398, 1226, 1130, 1097, 611. $^1$H NMR (400 MHz, $CDCl_3$): δ (ppm) 1.62 (s, 3H, $CH_3$), 4.24 (s, 2H, $CH_2$), 5.46 (s, 1H, CH), 7.27 (m, 5H, ArH), 7.53 (d, 2H, *J* = 8.8 Hz), 7.89 (d, 2H, *J* = 8.7 Hz); $^{13}$C NMR (100 MHz, $CDCl_3$): δ (ppm) 28.5, 36.4, 64.3, 77.3, 128.3, 128.5, 128.6, 129.4, 129.7, 129.8, 129.9, 130.0, 130.3, 131.9, 134.7, 136.5, 163.2, 194.1, 196.6. Anal. calcd. for $C_{19}H_{16}ClNO_3S_2$: C, 56.22; H, 3.97; N, 3.45. Found: C, 56.41; H, 4.021; N, 3.15.

**2-(Benzylthio)-4-(2-(4-bromophenyl)-1-hydroxy-2-oxoethyl)-4-methylthiazol-5(4*H*)-one (4Br-Ala).** Yield 79%, m.p. 147–150 °C, FT-IR (KBr): ν ($cm^{-1}$) 3423, 3035, 2920, 1732, 1618, 1375, 1256, 1062, 631. $^1$H NMR (400 MHz, $CDCl_3$): δ (ppm) 1.52 (s, 3H, $CH_3$), 4.24 (s, 2H, $CH_2$), 5.42 (s, 1H, CH), 7.27 (m, 5H, ArH), 7.66 (d, 2H, *J* = 8.6 Hz), 7.96 (d, 2H, *J* = 8.7 Hz); $^{13}$C NMR (100 MHz, $CDCl_3$): δ (ppm) 27.0, 38.7, 63.3, 79.6, 124.9, 128.3, 128.3, 128.8, 129.3, 129.6, 130.3, 130.7, 131.3, 132.1, 132.4, 134.9, 162.6, 193.2, 196.9. Anal. calcd. for $C_{19}H_{16}BrNO_3S_2$: C, 50.67; H, 3.58; N, 3.11. Found: C, 50.40; H, 4.25; N, 3.36.

**2-(Benzylthio)-4-(1-hydroxy-2-(4-nitrophenyl)-2-oxoethyl)-4-methylthiazol-5(4*H*)-one (4$NO_2$-Ala).** Yield 86%, m.p. 113–114 °C, FT-IR (KBr): ν ($cm^{-1}$) 3415, 3052, 2923, 1721, 1622, 1384, 1269, 1115, 619. $^1$H NMR (400 MHz, $CDCl_3$): δ (ppm) 1.59 (s, 3H, $CH_3$), 4.21 (s, 2H, $CH_2$), 5.59 (s, 1H, CH), 7.24 (m, 1H, ArH), 7.93 (m, 2H, ArH), 7.95 (m, 2H, ArH), 8.18 (d, 2H, *J* = 8 Hz), 8.22 (d, 2H, *J* = 8.1 Hz); $^{13}$C NMR (100 MHz, $CDCl_3$): δ (ppm) 26.4, 37.7, 62.6, 79.0, 117.3, 117.5, 128.6, 128.8, 128.9, 129.4, 129.7, 130.4, 130.4, 131.7, 134.9, 140.5, 162.2, 193.6, 196.8. Anal. calcd. for $C_{19}H_{16}N_2O_5S_2$: C, 54.80; H, 3.87; N, 6.73. Found: C, 54.64; H, 3.71; N, 6.82.

**2-(Benzylthio)-4-(1-hydroxy-2-oxo-2-phenylethyl)-4-isobutylthiazol-5(4*H*)-one (4H-Leu).** Yield 69%, m.p. 113–117 °C, FT-IR (KBr): ν ($cm^{-1}$) 3405, 3020, 2928, 2862, 1714, 1627, 1453, 1375, 1273, 1238, 1119, 706. $^1$H NMR (400 MHz, $CDCl_3$): *δ (ppm)* 0.91 (d, 6H, *J* = 6.8 Hz), 1.52 (m, 1H, CH), 1.74 (d, 2H, *J* = 8.4 Hz), 4.28 (s, 2H, $CH_2$), 5.56 (s, 1H, CH), 7.28 (m, 5H, ArH), 7.96 (m, 5H, ArH); $^{13}$C NMR (100 MHz, $CDCl_3$): δ (ppm) 22.6, 22.6, 26.1, 36.9, 43.4, 64.3, 80.3, 127.8, 127.8, 128.3, 128.4, 129.2, 129.3, 130.1, 130.1, 132.5, 135.2, 163.7, 195.3, 198.8. Anal. calcd. for $C_{22}H_{23}NO_3S_2$: C, 63.90; H, 5.61; N, 3.39 Found: C, 64.12; H, 5.78; N, 3.19.

**2-(Benzylthio)-4-(2-(4-fluorophenyl)-1-hydroxy-2-oxoethyl)-4-isobutylthiazol-5(4*H*)-one (4F-Leu).** Yield 67%, m.p. 149–153 °C, FT-IR (KBr): ν ($cm^{-1}$) 3462, 3055, 2973, 1688, 1568, 1448, 1382, 1209, 1231, 1109, 641. $^1$H NMR (400 MHz, $CDCl_3$): δ (ppm) 0.91 (d, 6H, *J* = 6.6 Hz), 1.52 (m, 1H, CH), 1.73 (d, 2H, *J* = 8.06 Hz), 4.21 (s, 2H, $CH_2$), 5.44 (s, 1H, CH), 7.32 (m, 5H, ArH), 7.36 (m, 5H, ArH), 7.46 (d, 2H, *J* = 8.7 Hz), 7.91 (d, 2H, *J* = 8.8 Hz); $^{13}$C NMR (100 MHz, $CDCl_3$): *δ* (ppm) 22.5, 22.6, 27.0, 37.9, 42.4, 63.5, 78.3, 128.3, 128.4, 129.7, 129.8, 130.1, 131.5, 131.6, 132.4, 132.6, 133.1, 135.2, 136.6, 165.2, 195.3, 198.1. Anal. calcd. for $C_{22}H_{22}FNO_3S_2$: C, 61.23; H, 5.14; N, 3.25. Found: C, 61.55; H, 5.32; N, 3.37.

**2-(Benzylthio)-4-(2-(4-chlorophenyl)-1-hydroxy-2-oxoethyl)-4-isobutylthiazol-5(4*H*)-one (4Cl-Leu).** Yield

64%, m.p. 176–178 °C, FT-IR (KBr): ν ($cm^{-1}$) 3365, 3033, 2969, 1681, 1588, 1429, 1384, 1221, 1132, 1085, 613. $^1$H NMR (400 MHz, $CDCl_3$): δ (ppm) 0.91 (d, 6H, *J* = 6.8 Hz), 1.53 (m, 1H, CH), 1.72 (d, 2H, *J* = 8.4 Hz), 4.21 (s, 2H, $CH_2$), 5.39 (s, 1H, CH), 7.27 (m, 5H, ArH), 7.33 (m, 5H, ArH), 7.73 (d, 2H, *J* = 12.8 Hz), 7.87 (d, 2H, *J* = 8.8 Hz); $^{13}$C NMR (100 MHz, $CDCl_3$): δ (ppm) 21.8, 21.9, 25.7, 34.8, 40.6, 61.38, 77.8, 126.3, 126.5, 127.6, 128.1, 128.2, 129.6, 129.8, 130.5, 130.7, 131.9, 136.3, 163.1, 194.9, 197.3. Anal. calcd. for $C_{22}H_{22}ClNO_3S_2$: C, 58.98; H, 4.95; N, 3.13. Found: C, 59.26; H, 5.15; N, 3.34.

**2-(Benzylthio)-4-(2-(4-bromophenyl)-1-hydroxy-2-oxoethyl)-4-isobutylthiazol-5(4*H*)-one (4Br-Leu).** Yield 73%, m.p. 141–144 °C, FT-IR (KBr): ν ($cm^{-1}$) 3431, 3039, 2910, 1727, 1624, 1453, 1432, 1365, 1247, 1106, 1062, 623. $^1$H NMR (400 MHz, $CDCl_3$): δ (ppm) 0.93 (d, 6H, *J* = 6.8 Hz), 1.54 (m, 1H, CH), 1.64 (d, 2H, *J* = 8.4 Hz), 4.31 (s, 2H, $CH_2$), 5.38 (s, 1H, CH), 7.34 (m, 5H, ArH), 7.36 (m, 5H, ArH), 7.66 (d, 2H, *J* = 8.21 Hz), 7.97 (d, 2H, *J* = 7.56 Hz); $^{13}$C NMR (100 MHz, $CDCl_3$): δ (ppm) 21.5, 21.6, 26.7, 26.8, 42.6, 62.6, 75.1, 124.9, 126.5, 126.6, 127.3, 131.2, 131.3, 132.4, 132.5, 133.4, 133.6, 134.1, 136.8, 164.7, 195.7, 195.3, 194.5. Anal. calcd. for $C_{22}H_{22}BrNO_3S_2$: C, 53.66; H, 4.50; N, 2.84. Found: C, 53.85; H, 4.40; N, 3.12.

**2-(Benzylthio)-4-(1-hydroxy-2-(4-nitrophenyl)-2-oxoethyl)-4-isobutylthiazol-5(4*H*)-one (4$NO_2$-Leu).** Yield 58%, m.p. 121–125 °C, FT-IR (KBr): ν ($cm^{-1}$) 3418, 3052, 2929, 1725, 1628, 1441, 1369, 1274, 1171, 611. $^1$H NMR (400 MHz, $CDCl_3$): 1.01 (d, 6H, *J* = 6.65 Hz), 1.63 (m, 1H, CH), 1.82 (d, 2H, *J* = 8 Hz), 4.38 (s, 2H, $CH_2$), 5.36 (s, 1H, CH), 7.20 (m, 5H, ArH), 7.23 (m, 5H, ArH), 7.97 (d, 2H, *J* = 8.8 Hz), 8.21 (d, 2H, *J* = 8.4 Hz); $^{13}$C NMR (100 MHz, $CDCl_3$): δ (ppm) 23.9, 24.1, 28.3, 38.7, 44.1, 65.8, 79.6, 117.2, 117.3, 126.5, 126.7, 128.3, 128.4, 129.2, 131.4, 131.5, 133.4, 137.6, 140.6, 164.7, 191.8, 194.6. Anal. calcd. for $C_{22}H_{23}N_2O_5S_2$: C, 57.63; H, 4.84; N, 6.11. Found: C, 57.50; H, 4.64; N, 6.37.

# 4. Computational Study of the Products

## 4. 1. Method

All computations were carried out with the Gaussian 09 program package.[30] The energies and geometries were calculated with B3LYP method[31,32] and 6-311++G(d,p) basis set. Harmonic vibrational frequencies were computed to confirm an optimized geometry corresponding to the local minimum that has only real frequencies. NMR spectra have been calculated at B3LYP/6–311++G(d,p) level of theory in $CDCl_3$ solvent using the gauge-independent atomic orbital (GIAO) method.[33] UV-visible spectra were calculated theoretically in $CDCl_3$ solvent as well as gas phase using time-dependent (TD) DFT method with B3LYP level of theory and 6–311++G(d,p) basis set based on the previously optimized ground state geometry of the products.[34,35]

## 4. 2. Geometrical Analysis

First of all, to find the most stable geometries of the compounds we done optimization calculations on the molecular structures of the synthesized compounds which are verified with IR and NMR spectroscopic techniques. Then for verifying that the optimized structures are true minima we calculated the vibrational frequencies of them. The results showed that all of the calculated frequencies for all compounds have positive values verifying that all structures are true minima. The optimized structures of the products are shown in column 2 of Table 1. In addition, some selected most important geometrical data of all products are collected in Tables 2a, 2b, and 2c. The atom numbered model structure of each of the 4X-Gly, 4X-Ala, and 4X-Leu products are included in Tables 2a, 2b and 2c, respectively.

The results of the geometry optimization of 4X-Gly derivatives proved our proposed (*Z*) stereochemistry of the conjugated C=C double bond. This stereochemistry let the conjugation spread longer through the whole molecule from the X substituted phenyl ring to the thiazolone carbonyl double bond and enabled the products to absorb UV-visible light in the visible area as we will discuss later. The results also revealed that there are no significant differences in the geometrical characteristics of the products with different X substituents and almost all of them have nearly the same geometrical structures with some small differences in bond lengths and/or angles. Calculated dihedral angles also revealed that the whole molecular structure of the products is not planar but the un-planarity is not too large to prevent conjugation.

The 4X-Ala and 4X-Leu products have the same optimized geometrical structures because they both have hydroxyl functional groups attached to the carbon atoms between carbonyl groups instead of a C=C double bond; therefore in these cases we do not have a longer conjugation system as we see in 4X-Gly products. These structural differences make some differences from the structural and chemical reactivity point of view between the 4X-Ala and 4X-Leu with 4X-Gly products.

Unlike the 4X-Gly products the optimization calculations revealed that the 4X-Ala and 4X-Leu products have one intramolecular hydrogen bond which is located between the hydroxyl group and the oxygen atom of the carbonyl group. Hydrogen bond characterization data of these two groups are included in Table 1. This intramolecular hydrogen bond makes the products more stable and also more rigid than that of 4X-Gly products. Observed intramolecular hydrogen bond lengths and angles varied from 2.154 to 2.195 Å and 133.05° to 134.50° which is in accordance with nearly strong hydrogen bonds. As

**Tables 2a.** Optimized geometrical data of 4X-Gly products.

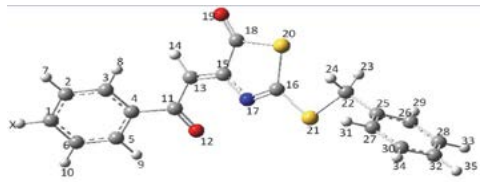

| X | H | F | Cl | Br | $NO_2$ |
|---|---|---|---|---|---|
| Bond length/(Å) | | | | | |
| $C_4$–$C_{11}$ | 1.500 | 1.499 | 1.501 | 1.501 | 1.509 |
| C11–C13 | 1.490 | 1.489 | 1.487 | 1.487 | 1.482 |
| C11–O12 | 1.218 | 1.218 | 1.218 | 1.218 | 1.217 |
| C13–C15 | 1.351 | 1.351 | 1.352 | 1.352 | 1.354 |
| C13–H14 | 1.084 | 1.084 | 1.084 | 1.084 | 1.083 |
| C15–C18 | 1.513 | 1.513 | 1.514 | 1.515 | 1.517 |
| C15–N17 | 1.376 | 1.376 | 1.375 | 1.374 | 1.370 |
| N17–C16 | 1.286 | 1.286 | 1.287 | 1.287 | 1.289 |
| C16–S20 | 1.799 | 1.799 | 1.798 | 1.798 | 1.797 |
| C18–S20 | 1.833 | 1.833 | 1.833 | 1.833 | 1.832 |
| C18–O19 | 1.196 | 1.196 | 1.196 | 1.196 | 1.195 |
| C16–S21 | 1.751 | 1.750 | 1.745 | 1.745 | 1.746 |
| S21–C22 | 1.858 | 1.858 | 1.858 | 1.858 | 1.859 |
| Angle/(°) | | | | | |
| C4–C11–O12 | 121.23 | 121.03 | 120.81 | 120.76 | 120.05 |
| C4–C11–C13 | 117.42 | 117.47 | 117.46 | 117.46 | 117.33 |
| C11–C13–C15 | 125.58 | 125.58 | 125.68 | 125.72 | 125.78 |
| C13–C15–N17 | 127.15 | 127.25 | 127.37 | 127.41 | 127.61 |
| H14–C13–C15 | 116.20 | 116.09 | 115.97 | 115.92 | 115.87 |
| C15–C18–C19 | 118.59 | 128.68 | 128.67 | 128.67 | 128.53 |
| C15–C18–S20 | 106.78 | 106.79 | 106.81 | 106.80 | 106.83 |
| N17–C16–S20 | 117.86 | 117.87 | 117.89 | 117.90 | 117.94 |
| N17–C16–S21 | 119.52 | 119.51 | 119.48 | 119.47 | 119.37 |
| C16–S21–C22 | 103.64 | 103.67 | 103.62 | 103.68 | 103.76 |
| Dihedral/(°) | | | | | |
| C3–C4–C11–C13 | –13.22 | –12.49 | –13.02 | –13.42 | –17.95 |
| C4–C11–C13–C15 | 147.88 | 149.30 | 152.09 | 153.32 | 158.11 |
| O12–C11–C13–C15 | –33.94 | –32.45 | –29.66 | –28.46 | –23.56 |
| C13–C15–C18–S20 | –179.38 | –179.17 | –179.10 | –178.81 | –179.47 |
| S20–C16–S21–C22 | 0.820 | 0.207 | –0.002 | –0.448 | 0.291 |

we discussed about 4X-Gly products in the case of 4X-Ala and 4X-Leu products also structural characteristics such as bond length, angles and dihedral angles do not show obvious differences within the products of each type with various X substituents. As the dihedral angles showed both of the 4X-Ala and 4X-Leu products are not planar same as the 4X-Gly ones. Another structural feature of 4X-Ala and 4X-Leu products is that the carbonyl functional group is directed to the center of the thiazolactone ring at all of the X substituted derivatives of them.

## 4. 3. UV-Visible Spectra Prediction

In this part, we get help from chemical computational methods to get information about the UV-visible light absorption capability of the products. Therefore, the optimized ground state geometry of the synthesized products have been submitted to the calculation of the UV-visible spectra using the time-dependent (TD) DFT method at B3LYP/6–311++G(d,p) computational level in both gas and solution phase. "Time-dependent density functional theory (TD-DFT)[36] has recently emerged as a powerful tool for investigating the static and dynamic properties of the molecules in their excited states, allowing for the best compromise between accuracy and computational cost."[37] The calculated absorption maxima ($\lambda_{max}$) are a function of the electron availability for the synthesized compounds and their corresponding oscillator strengths are listed in Table 3.

Figure 1 shows the resulting absorption spectra for each type of the synthesized compounds over the wave-

**Tables 2b.** Optimized geometrical data of 4X-Ala products.

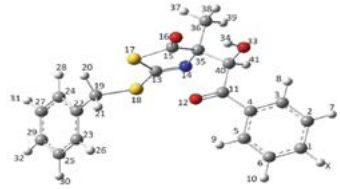

| X | H | F | Cl | Br | $NO_2$ |
|---|---|---|---|---|---|
| Bond length/(Å) | | | | | |
| C4–C11 | 1.492 | 1.490 | 1.491 | 1.492 | 1.500 |
| C11–O12 | 1.217 | 1.217 | 1.217 | 1.217 | 1.214 |
| C11–C40 | 1.545 | 1.545 | 1.545 | 1.545 | 1.543 |
| C40–O33 | 1.422 | 1.422 | 1.422 | 1.422 | 1.422 |
| C40–C35 | 1.553 | 1.552 | 1.552 | 1.552 | 1.551 |
| C35–C15 | 1.542 | 1.542 | 1.542 | 1.542 | 1.542 |
| C15–O16 | 1.201 | 1.201 | 1.201 | 1.201 | 1.201 |
| C35–N14 | 1.448 | 1.448 | 1.449 | 1.448 | 1.448 |
| C35–C36 | 1.545 | 1.545 | 1.545 | 1.545 | 1.545 |
| N14–C13 | 1.270 | 1.270 | 1.270 | 1.270 | 1.271 |
| C13–S17 | 1.805 | 1.806 | 1.806 | 1.806 | 1.806 |
| C13–S18 | 1.768 | 1.768 | 1.768 | 1.767 | 1.766 |
| S17–C15 | 1.817 | 1.815 | 1.815 | 1.815 | 1.814 |
| S18–C19 | 1.858 | 1.858 | 1.859 | 1.858 | 1.858 |
| Angle/(°) | | | | | |
| C5–C4–C11 | 118.01 | 118.04 | 118.06 | 118.09 | 122.58 |
| C4–C11–O12 | 121.61 | 121.54 | 121.43 | 121.39 | 120.97 |
| C4–C11–C40 | 118.55 | 118.40 | 118.44 | 118.46 | 118.31 |
| C40–C35–C15 | 110.96 | 110.84 | 110.81 | 110.85 | 110.88 |
| C35–C15–O16 | 126.27 | 126.17 | 126.12 | 126.15 | 126.07 |
| C35–C40–O33 | 112.70 | 112.63 | 112.69 | 112.71 | 112.96 |
| C15–C35–N14 | 109.64 | 109.64 | 109.65 | 109.65 | 109.66 |
| C15–C35–C36 | 107.54 | 107.59 | 107.62 | 107.59 | 107.59 |
| C15–S17–C13 | 87.97 | 87.98 | 87.99 | 87.99 | 87.99 |
| S17–C13–S18 | 121.60 | 121.51 | 121.49 | 121.56 | 121.65 |
| C13–S18–C19 | 103.58 | 103.52 | 103.46 | 103.58 | 103.74 |
| Dihedral/(°) | | | | | |
| C4–C11–C40–O33 | –73.66 | –71.73 | –71.80 | –71.55 | –72.79 |
| C11–C40–C35–C15 | 60.29 | 60.20 | 60.12 | 59.94 | 60.81 |
| C40–C35–C15–O16 | 50.44 | 49.99 | 50.15 | 50.05 | 49.71 |
| C36–C35–C40–O33 | 55.34 | 55.11 | 55.15 | 54.95 | 56.05 |
| S17–C13–S18–C19 | –8.81 | –10.13 | –13.24 | –12.12 | –5.46 |

length range of 200–800 nm in both the gas and solution phases which are obtained using the above-mentioned calculation methods. Analysis of the obtained plots for each class of the synthesized compounds from the absorption maxima ($\lambda_{max}$) and intensity points of view clearly point to the following results:

1. All of the products have absorption bands in the range of 250–350 nm because of the presence of a phenyl ring in all structures.
2. The absorption spectra of 4X-Gly products show the two absorption bands in which the absorption maxima are located in visible light range as expected because of the long conjugated π system present in their structure.
3. The absorption spectra of 4X-Ala and 4X-Leu products do not have an absorption band in the range of visible light because they lack a long conjugated π system and show only one absorption band in the ultraviolet region.
4. The calculated UV-visible spectrum for each product in the solution phase has a higher intensity than that of its gas phase for all compounds.
5. Absorption maxima for 4X-Gly, 4X-Ala, and 4X-Leu compounds in solution phase range from 481–494, 262–297, and 260–293 nm, respectively.
6. The absorption maxima order in the case of 4X-Gly products is: $4NO_2 > 4Br > 4Cl > 4F > 4H$.
7. Substituting the F, Cl, Br and $NO_2$ groups instead of a hydrogen atom at the *para* position of the phenyl ring

**Tables 2c.** Optimized geometrical data of 4X-Leu products.

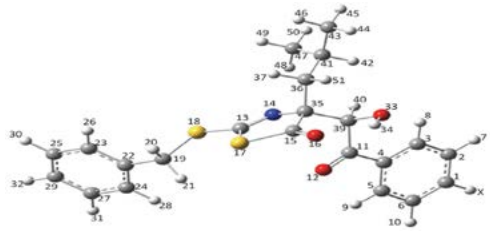

| X | H | F | Cl | Br | $NO_2$ |
|---|---|---|---|---|---|
| Bond length/(Å) | | | | | |
| C4–C11 | 1.493 | 1.491 | 1.492 | 1.493 | 1.501 |
| C11–O12 | 1.217 | 1.217 | 1.217 | 1.216 | 1.214 |
| C11–C39 | 1.546 | 1.546 | 1.545 | 1.545 | 1.544 |
| C39–O33 | 1.422 | 1.422 | 1.422 | 1.422 | 1.422 |
| C39–C35 | 1.552 | 1.552 | 1.551 | 1.552 | 1.551 |
| C35–N14 | 1.448 | 1.448 | 1.449 | 1.448 | 1.448 |
| N14–C13 | 1.269 | 1.269 | 1.270 | 1.270 | 1.270 |
| C13–S17 | 1.804 | 1.804 | 1.805 | 1.805 | 1.806 |
| C13–S18 | 1.768 | 1.768 | 1.768 | 1.768 | 1.767 |
| S18–C19 | 1.858 | 1.858 | 1.858 | 1.858 | 1.859 |
| S17–C15 | 1.815 | 1.815 | 1.815 | 1.815 | 1.812 |
| C15–O16 | 1.201 | 1.201 | 1.201 | 1.201 | 1.202 |
| C15–C35 | 1.546 | 1.546 | 1.542 | 1.546 | 1.546 |
| C35–C36 | 1.563 | 1.563 | 1.561 | 1.564 | 1.564 |
| Angle/(°) | | | | | |
| C5–C4–C11 | 117.99 | 117.98 | 118.08 | 118.04 | 122.71 |
| C4–C11–O12 | 121.48 | 121.40 | 121.34 | 121.30 | 120.82 |
| C11–C39–O33 | 109.16 | 109.14 | 108.67 | 109.09 | 108.68 |
| O12–C11–C39 | 120.05 | 120.23 | 120.24 | 120.33 | 120.94 |
| C11–C39–C35 | 112.53 | 112.64 | 112.55 | 112.64 | 112.85 |
| C39–C35–C15 | 110.25 | 110.23 | 110.33 | 110.26 | 110.16 |
| C35–C15–O16 | 126.11 | 126.07 | 126.14 | 126.06 | 125.92 |
| C15–C35–N14 | 109.17 | 109.17 | 109.41 | 109.18 | 109.18 |
| C36–C35–C39 | 111.24 | 111.20 | 111.95 | 111.14 | 111.18 |
| C35–C15–S17 | 108.75 | 108.74 | 108.72 | 108.76 | 108.80 |
| N14–C13–S17 | 118.25 | 118.24 | 118.23 | 118.21 | 118.14 |
| C13–S18–C19 | 103.57 | 103.63 | 103.61 | 103.60 | 103.66 |
| S17–C13–S18 | 121.59 | 121.59 | 121.57 | 121.60 | 121.58 |
| Dihedral/(°) | | | | | |
| C4–C11–C39–O33 | –72.01 | –70.47 | –72.16 | –70.89 | –70.30 |
| C4–C11–C39–C35 | 162.26 | 163.66 | 162.28 | 163.26 | 163.89 |
| C11–C39–C35–C15 | 58.67 | 58.40 | 59.88 | 58.76 | 50.01 |
| O33–C39–C35–C36 | 51.23 | 50.81 | 54.48 | 51.27 | 51.78 |
| O16–C15–C35–C36 | –68.98 | –69.37 | –70.96 | –69.48 | –69.97 |
| S17–C13–S18–C19 | –10.64 | –8.93 | –10.17 | –7.28 | –8.33 |

**Table 3.** Calculated absorption maxima ($\lambda_{max}$) and corresponding oscillator strength of the products.

| **Comp.** | **4X-Gly** | | | | **4X-Ala** | | | | **4X-Leu** | | | |
|---|---|---|---|---|---|---|---|---|---|---|---|---|
| **phase** | **Gas** | | **$CH_3CN$** | | **Gas** | | **$CH_3CN$** | | **Gas** | | **$CH_3CN$** | |
| **X** | **λ/nm** | ***f*** | **λ/nm** | ***f*** | **λ/nm** | ***f*** | **λ/nm** | ***f*** | **λ/nm** | ***f*** | **λ/nm** | ***f*** |
| H | 457.79 | 0.3795 | 481.89 | 0.4854 | 291.41 | 0.0542 | 274.05 | 0.0945 | 253.99 | 0.1721 | 260.93 | 0.3160 |
| F | 462.32 | 0.3856 | 484.43 | 0.4916 | 257.02 | 0.3040 | 262.10 | 0.2732 | 257.24 | 0.3096 | 262.82 | 0.2906 |
| Cl | 467.38 | 0.4223 | 488.76 | 0.5470 | 288.52 | 0.2724 | 287.65 | 0.2960 | 270.64 | 0.2140 | 277.82 | 0.2619 |
| Br | 471.95 | 0.4229 | 488.87 | 0.5707 | 295.09 | 0.4917 | 297.15 | 0.3445 | 277.18 | 0.3763 | 283.56 | 0.4633 |
| $NO_2$ | 465.84 | 0.4002 | 494.26 | 0.5086 | 302.93 | 0.0187 | 292.66 | 0.5185 | 303.31 | 0.0182 | 293.52 | 0.5116 |

resulted in redshift effects at UV-visible absorption behavior of the 4X-Gly products and the $4NO_2$ group showed the highest redshift value among all of the substituting groups.

The lower wavelength absorption band appeared for the 4X-Gly products and also the only absorption band of the 4X-Ala and 4X-Leu products correspond to the electronic transitions among the aromatic rings which are mainly derived from the contribution of π–π* bands. And the visible absorption maxima of the 4X-Gly products correspond to the electron transition from the highest occupied molecular orbital (HOMO) to the lowest unoccupied molecular orbital (LUMO).

## 4. 4. NMR Spectra

The most powerful analytical tool for structural elucidation of organic compounds is Nuclear magnetic resonance (NMR) spectroscopy.[38] In addition to the recording of the experimental $^1$H NMR spectra for the products in chloroform ($CDCl_3$) using Bruker AMX 400 MHz spectrometer we have employed the gauge-independent atomic orbital (GIAO) method[33,39] at B3LYP/6–311++G(d,p) level of theory in $CDCl_3$ solvent to calculate the chemical shielding of each atom in the ground state optimized geometry of the products. The theoretical $^1$H NMR chemical shift values for the products in $CDCl_3$ solvent are listed in Table 4. We also includ some of the experimental $^1$H NMR chemical shift values for comparison.

To get $^1$H NMR chemical shift of the products on the TMS scale we first calculated the isotropic shielding values for tetramethylsilane (TMS) protons using the same model which was used in the case of the products in chloroform ($CDCl_3$) solvent and 31.9707 ppm was determined as the $^1$H NMR chemical shift of the 12 equivalent protons of TMS. With the absolute chemical shift of the TMS protons in hand, the real chemical shift of each proton of the products was obtained using $\delta_{rel}(Hx) = \delta(TMS) - \delta(Hx)$ equation where

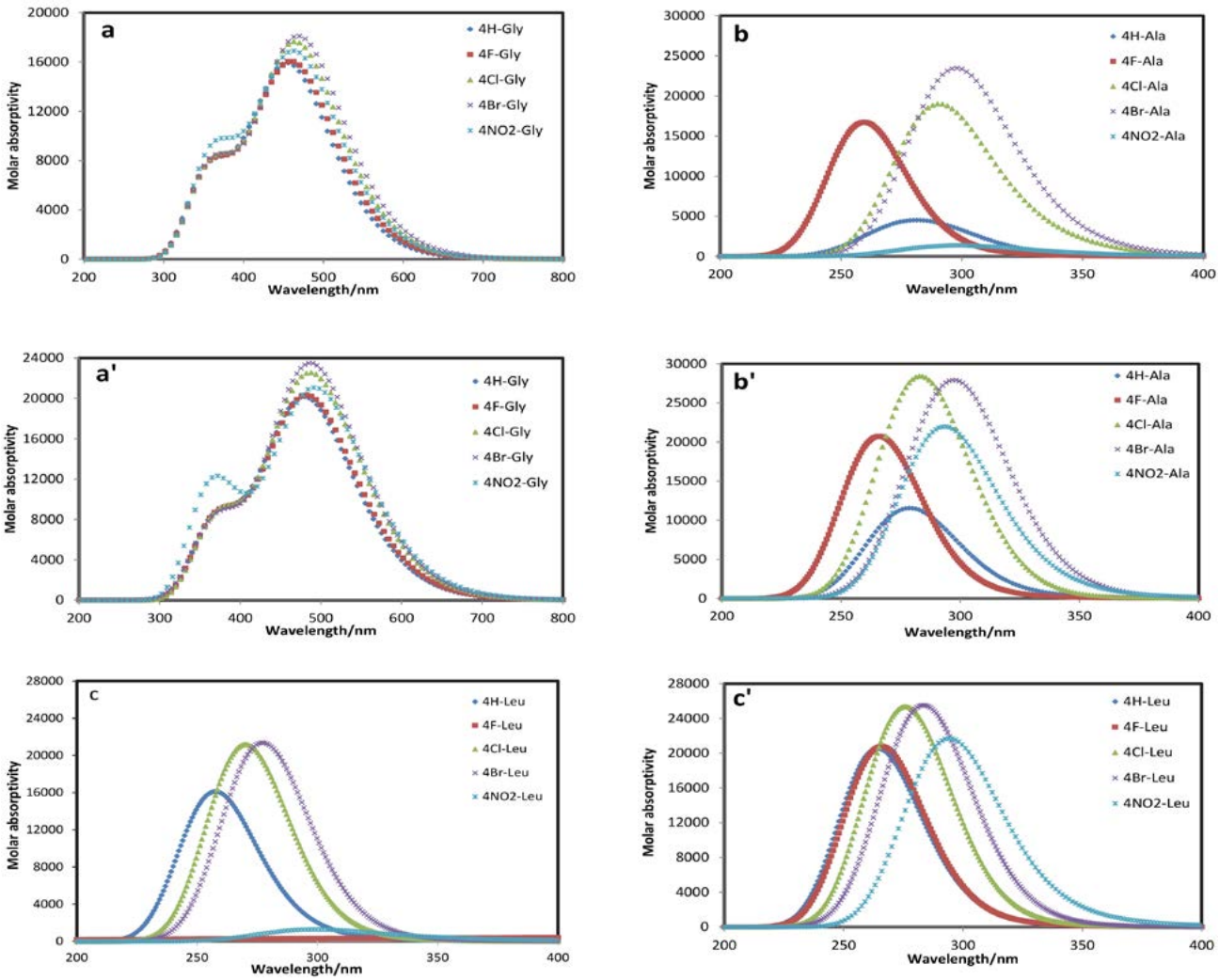


**Figure 1.** Calculated UV-visible spectra for the synthesized products. 4X-Gly (a: gas; a': $CH_3CN$), 4X-Ala (b: gas; b': $CH_3CN$) and 4X-Leu (c: gas; c': $CH_3CN$).

$\delta_{rel}$(Hx) is the real chemical shift of the proton x, δ(Hx) is the absolute shielding of the proton x and δ(TMS) is the absolute shielding of the TMS equivalent protons. From the results collected in Table 4, it is clear that there is a good agreement between theoretically calculated chemical shifts and the experimental data for protons of the products. Figure 2 presents this correlation, showing the calculated chemical shifts versus computed ones for some protons of $4NO_2$-Gly, $4NO_2$-Ala, and $4NO_2$-Leu derivatives of the synthesized products.

The same correlation as depicted on Figure 2 could be found in the case of the other derivatives of all three classes of the products which are not shown here.

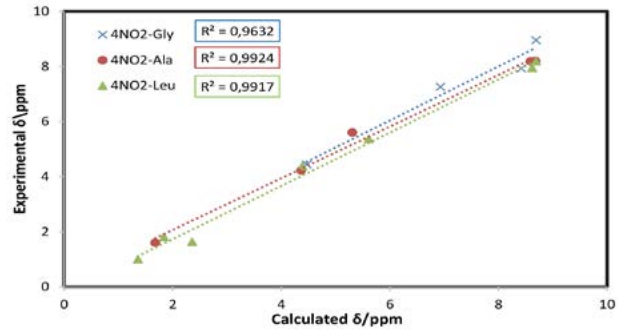


**Figure 2.** Correlation between calculated and experimental chemical shifts.

**Table 4**. Theoretical $^1$H isotropic chemical shifts (with respect to TMS, all values in ppm) for the products obtained at B3LYP/6–311++G(d,p) level of theory (some experimental data are shown in *italic* for comparison).

| **Atom number** | **4H-Gly** | **4F-Gly** | **4Cl-Gly** | **4Br-Gly** | **$4NO_2$-Gly** |
|---|---|---|---|---|---|
| H7, H10 | 7.80 | 7.42 | 7.74 | 7.81 | 8.69 |
| H8, H9 | 8.37 | 8.37 | 8.29 | 8.26 | 8.42 |
| H(X) | 7.91 | — | — | — | — |
| H14 | 7.42 | 7.34 | 7.32 | 7.31 | 7.26 |
| *H14* | *7.13* | *6.87* | *6.89* | *6.89* | *6.93* |
| H23, H24 | 4.42 | 4.42 | 4.43 | 4.44 | 4.47 |
| *H23, H24* | *4.68* | *4.44* | *4.44* | *4.42* | *4.44* |
| H29, H31 | 7.81 | 7.80 | 7.81 | 7.81 | 7.81 |
| H33, H34 | 7.73 | 7.73 | 7.73 | 7.74 | 7.75 |
| H35 | 7.68 | 7.68 | 7.69 | 7.69 | 7.70 |
| **Atom number** | **4H-Ala** | **4F-Ala** | **4Cl-Ala** | **4Br-Ala** | **$4NO_2$-Ala** |
| H8, H9 | 8.17 | 8.53 | 8.44 | 8.40 | 8.59 |
| H7, H10 | 8.20 | 7.42 | 7.74 | 7.81 | 8.68 |
| H(X) | 7.91 | — | — | — | — |
| H41 | 5.39 | 5.34 | 5.33 | 5.32 | 5.31 |
| *H41* | *5.44* | *5.44* | *5.46* | *5.42* | *5.60* |
| H34 | 3.35 | 3.41 | 3.40 | 3.37 | 3.57 |
| H37, H38, H39 | 1.67 | 1.66 | 1.65 | 1.65 | 1.68 |
| *H37, H38, H39* | *1.57* | *1.55* | *1.63* | *1.52* | *1.60* |
| H20, H21 | 4.36 | 4.38 | 4.36 | 4.36 | 4.37 |
| *H20, H21* | *4.23* | *4.22* | *4.24* | *4.24* | *4.22* |
| H26, H28 | 7.76 | 7.78 | 7.76 | 7.76 | 7.76 |
| H30, H31 | 7.68 | 7.70 | 7.68 | 7.68 | 7.69 |
| H32 | 7.63 | 7.65 | 7.63 | 7.63 | 7.64 |
| **Atom number** | **4H-Leu** | **4F-Leu** | **4Cl-Leu** | **4Br-Leu** | **$4NO_2$-Leu** |
| H8, H9 | 8.54 | 8.54 | 8.44 | 8.41 | 8.62 |
| H7, H10 | 7.81 | 7.42 | 7.76 | 7.82 | 8.69 |
| H(X) | 7.95 | — | — | — | — |
| H40 | 5.69 | 5.61 | 5.56 | 5.59 | 5.61 |
| *H40* | *5.57* | *5.44* | *5.40* | *5.39* | *5.37* |
| H34 | 3.41 | 3.38 | 3.62 | 3.44 | 3.62 |
| H37, H51 | 1.76 | 1.76 | 1.72 | 1.76 | 1.84 |
| *H37, H51* | *1.73* | *1.72* | *1.71* | *1.63* | *1.81* |
| H42 | 2.38 | 2.35 | 2.16 | 2.36 | 2.36 |
| *H42* | *1.52* | *1.52* | *1.53* | *1.50* | *1.63* |
| H44–46, H48–50 | 1.07 | 1.38 | 1.13 | 1.07 | 1.36 |
| *H44–46, H48–50* | *0.90* | *0.90* | *0.91* | *0.92* | *1.00* |
| H20, H21 | 4.38 | 4.37 | 4.37 | 4.37 | 4.39 |
| *H20, H21* | *4.29* | *4.22* | *4.21* | *4.32* | *4.39* |
| H26, H28 | 7.78 | 7.78 | 7.78 | 7.78 | 7.78 |
| H30, H31 | 7.70 | 7.70 | 7.70 | 7.70 | 7.70 |
| H32 | 7.65 | 7.65 | 7.65 | 7.65 | 7.65 |

## 4. 5. Atomic Net Charges

One of the most important and useful concepts which describe how the electron density is distributed within a molecule is atomic charges. Many theories, which could be applied to understand the structural characteristics of the molecules, make use of atomic charges as fundamental properties.[40] In addition, atomic charges of the molecules can be correlated with many observable characteristics of the molecules, such as electric potentials, dipole moments, polarizability, nuclear magnetic resonance chemical shifts,

**Table 5.** Mulliken and natural bond orbital (NBO) atomic charge distribution of the products calculated using B3LYP/6–311++G(d,p) level in gas phase.

| Atom number | 4H-Gly | | 4F-Gly | | 4Cl-Gly | | 4Br-Gly | | $4NO_2$-Gly | |
|---|---|---|---|---|---|---|---|---|---|---|
| | Mulliken | NBO | Mulliken | NBO | Mulliken | NBO | Mulliken | NBO | Mulliken | NBO |
| C4 | 1.450 | –0.140 | 1.469 | –0.153 | 1.488 | –0.141 | 1.453 | –0.139 | 1.483 | –0.102 |
| C11 | –0.641 | 0.509 | –0.620 | 0.507 | –1.125 | 0.505 | –0.717 | 0.504 | –1.006 | 0.501 |
| O12 | –0.192 | –0.521 | –0.193 | –0.523 | –0.194 | –0.521 | –0.184 | –0.521 | –0.177 | –0.511 |
| C13 | –0.065 | –0.204 | –0.093 | –0.209 | 0.002 | –0.212 | 0.030 | –0.213 | 0.098 | –0.228 |
| C15 | 0.450 | 0.709 | 0.478 | 0.083 | 0.545 | 0.086 | 0.483 | 0.087 | 0.608 | 0.099 |
| C18 | 0.030 | 0.406 | 0.034 | 0.406 | 0.017 | 0.406 | 0.018 | 0.406 | –0.030 | 0.405 |
| O19 | –0.241 | –0.514 | –0.240 | –0.513 | –0.237 | –0.512 | –0.237 | –0.512 | –0.230 | –0.507 |
| S20 | 0.200 | 0.215 | 0.197 | 0.218 | –0.200 | 0.218 | –0.197 | 0.218 | –0.190 | 0.225 |
| N17 | 0.250 | –0.499 | 0.250 | –0.499 | 0.250 | –0.498 | 0.251 | –0.498 | 0.252 | –0.499 |
| C16 | –0.183 | –0.055 | –0.185 | –0.055 | –0.218 | –0.055 | –0.194 | –0.055 | –0.255 | –0.055 |
| S21 | 0.205 | 0.378 | 0.206 | 0.381 | 0.229 | 0.383 | 0.212 | 0.384 | 0.245 | 0.394 |
| C22 | –0.729 | –0.502 | –0.736 | –0.502 | –0.717 | 0.502 | –0.739 | –0.502 | –0.729 | –0.501 |
| C25 | 0.659 | –0.070 | 0.661 | –0.071 | 0.663 | –0.071 | 0.660 | –0.071 | 0.660 | –0.072 |
| **Atom number** | **4H-Ala** | | **4F-Ala** | | **4Cl-Ala** | | **4Br-Ala** | | **$4NO_2$-Ala** | |
| | Mulliken | NBO | Mulliken | NBO | Mulliken | NBO | Mulliken | NBO | Mulliken | NBO |
| C4 | 1.191 | –0.154 | 1.253 | –0.168 | 0.524 | –0.151 | 1.446 | –0.148 | 1.044 | –0.115 |
| C11 | –0.475 | 0.558 | –0.469 | 0.556 | –0.367 | 0.554 | –0.750 | 0.554 | –0.260 | 0.556 |
| O12 | –0.102 | –0.552 | –0.100 | –0.553 | –0.106 | –0.552 | –0.085 | –0.551 | –0.081 | –0.537 |
| C40 | –0.273 | 0.066 | –0.301 | 0.065 | 0.255 | 0.065 | 0.286 | 0.065 | –0.133 | 0.063 |
| O33 | –0.086 | –0.725 | –0.088 | –0.726 | –0.087 | –0.726 | –0.086 | –0.726 | –0.078 | –0.725 |
| C35 | 0.421 | 0.003 | 0.413 | 0.003 | 0.440 | 0.003 | 0.423 | 0.003 | 0.423 | 0.003 |
| C15 | –0.293 | 0.445 | –0.310 | 0.443 | –0.300 | 0.443 | –0.295 | 0.443 | –0.291 | 0.441 |
| O16 | –0.217 | –0.563 | –0.217 | –0.563 | –0.214 | –0.563 | –0.214 | –0.563 | –0.208 | –0.562 |
| S17 | 0.145 | 0.237 | 0.154 | 0.239 | 0.135 | 0.240 | 0.157 | 0.239 | 0.176 | 0.243 |
| C13 | –0.408 | –0.036 | –0.397 | –0.036 | –0.395 | –0.036 | –0.393 | –0.036 | –0.401 | –0.037 |
| N14 | 0.098 | –0.520 | 0.103 | –0.523 | 0.100 | –0.522 | 0.103 | –0.523 | 0.111 | –0.527 |
| S18 | –0.086 | 0.324 | –0.087 | 0.325 | –0.097 | 0.324 | –0.104 | 0.324 | –0.095 | 0.329 |
| C19 | –0.655 | –0.500 | –0.646 | –0.499 | –0.642 | –0.499 | –0.691 | –0.499 | –0.633 | –0.499 |
| C22 | 0.606 | –0.066 | 0.603 | –0.067 | 0.621 | –0.007 | 0.663 | –0.067 | 0.554 | –0.068 |
| **Atom number** | **4H-Leu** | | **4F-Leu** | | **4Cl-Leu** | | **4Br-Leu** | | **$4NO_2$-Leu** | |
| | Mulliken | NBO | Mulliken | NBO | Mulliken | NBO | Mulliken | NBO | Mulliken | NBO |
| C4 | 0.972 | –0.154 | 1.031 | –0.169 | 0.170 | –0.170 | 0.520 | –0.193 | 0.787 | –0.164 |
| C11 | –0.578 | 0.560 | –0.582 | 0.530 | –0.504 | 0.290 | –0.477 | 0.297 | –0.365 | 0.296 |
| O12 | –0.077 | –0.551 | –0.075 | –0.554 | –0.095 | –0.569 | –0.083 | –0.571 | –0.060 | –0.558 |
| C39 | –0.373 | 0.059 | –0.404 | 0.159 | –0.162 | 0.241 | –0.179 | 0.452 | –0.134 | 0.442 |
| O33 | –0.024 | –0.725 | –0.027 | –0.741 | –0.029 | –0.862 | 0.027 | –0.895 | –0.016 | 0.897 |
| C35 | 0.920 | 0.016 | 0.920 | –0.012 | 0.511 | –0.128 | 1.004 | –0.180 | 1.033 | –0.184 |
| C36 | –0.436 | –0.365 | –0.376 | –0.368 | 0.225 | –0.386 | –0.378 | –0.406 | –0.441 | –0.406 |
| C15 | –0.261 | 0.447 | –0.286 | 0.445 | –0.442 | 0.441 | –0.270 | 0.425 | –0.271 | 0.423 |
| O16 | –0.185 | –0.565 | –0.185 | –0.565 | –0.178 | –0.562 | –0.182 | –0.571 | –0.177 | –0.571 |
| S17 | 0.183 | 0.239 | 0.203 | 0.240 | 0.168 | 0.242 | 0.187 | 0.230 | 0.204 | 0.236 |
| C13 | –0.581 | –0.034 | –0.576 | –0.034 | –0.395 | –0.034 | –0.591 | –0.041 | –0.564 | –0.042 |
| N14 | 0.282 | –0.529 | 0.281 | –0.532 | 0.280 | –0.538 | 0.278 | –0.550 | 0.285 | –0.559 |
| S18 | –0.134 | 0.322 | –0.128 | 0.323 | –0.097 | 0.324 | –0.136 | 0.321 | –0.146 | 0.323 |
| C19 | –0.674 | –0.499 | –0.665 | –0.499 | –0.631 | –0.499 | –0.678 | –0.501 | –0.678 | –0.500 |
| C22 | 0.570 | –0.065 | 0.543 | –0.066 | 0.509 | –0.067 | 0.525 | –0.067 | 0.532 | –0.068 |

electromagnetic spectra, vibrational spectra, and chemical reactivities.[40]

Making help of the atomic charges of the molecules to analyze and better understand their experimental data in favor of computational chemistry methods is usual and popular. Because the net charge of the whole molecule but not the atomic charges are accessible using experimental methods, determination of them by using computational chemistry methods could be so useful for many researchers to better understand the electron density distribution related property results of the interested molecules.[40]

Many methods to determine atomic charges exist; here we report the atomic charges on some important atoms of the studied molecules, which are obtained by the use of Milliken and natural bond orbital (NBO) analysis.

Both the Mullikan[41–43] and NBO[44] atomic charges are defined based on orbitals. The former one uses the sum of the electronic charge contributions of centered orbitals at each atom and half of the electronic overlap clouds between two atoms for each atom. But the latter one, uses electronic charge contributions of the orbitals which are orthogonalized and localized to form one or two center orbitals, so-called natural bond orbitals. Therefore, from the viewpoint of chemistry, natural bond orbital charge is more meaningful than the Mulliken charge.[40]

Some atomic charges for the products which were obtained using the B3LYP/6–311++G(d,p) method in the gas phase according to the natural bond orbital (NBO) analysis and also the Mulliken population are listed in Table 5.

Using NBO charges, C11 and C13 carbon atoms in 4X-Gly products have positive and negative charges, respectively. The amount of the positive charge on C11 increased with the increasing of the electron-withdrawing effect and also the polarizability of the substituent X from X = H to X = $NO_2$, therefore, the 4$NO_2$-Gly compound has the most positive C11 atom whereas the 4H-Gly compound has the lowest positive C11 atom.

The negative charge on the C13 atom is increased from X = H to X = $NO_2$ because the electron-withdrawing effect and polarizability of the substituent X diminished the electron-withdrawing effect of the benzoyl group and consequently on the C13 atom as well.

The NBO analysis revealed that the C4 atom of the 4X-Ala products shows the highest difference in its negative charge among the five products of that type. As evident for the C4 atom, the 4$NO_2$-Ala compound has the most negatively charged C4 atom.

Finally, NBO results showed that the charge on the C11 atom of the 4X-Leu products decreased with the increasing withdrawing effect and polarizability of the substituent X because of balancing of the electron-withdrawing effect of the oxygen atom due to its electronegativity with the withdrawing effect and polarizability of the substituent X attached to the phenyl ring.

## 4. 6. Electrostatic Potential Map

"Molecular electrostatic potential (MEP), *V*(r) at a given point r(x, y, z) in the vicinity of a molecule, is defined in terms of the interaction energy between the electrical charge generated from the molecule's electrons and nuclei and a positive test charge (a proton) located at (r)".[37] In this section, the molecular electrostatic potential (MEP) for the 4H-Gly, 4H-Ala and 4H-Leu products at the B3LYP/6–311++G(d,p) level are depicted in Figure 3. The electron-rich, neutral and electron-deficient regions around the specified molecule are presented by red, green and blue colors, respectively. Light blue and yellow colors represent the slightly electron-deficient and slightly electron-rich regions, respectively. Where the interaction energy between the electrical charges results in the strongest attractions, the surface appeared in blue; in contrast where it results in the strongest repulsion the surface appeared in red. Therefore, the electrostatic potential increases in the red < orange < yellow < green < blue order.[37]

Since molecular electrostatic potential was obtained based on the electronic density it could be applicable as a tool for evaluation of the electrophilic sites of the molecule and nucleophilic reactivity. In addition it is a useful descriptor for investigation of the non-covalent interactions such as hydrogen-bonding interactions.[37,45,46]

As seen from the Figure 3, the red regions of all three titled products are mainly localized around the oxygen atom of the carbonyl groups, therefore those are the most favorable sites for electrophilic attack. On the other hand, posi-

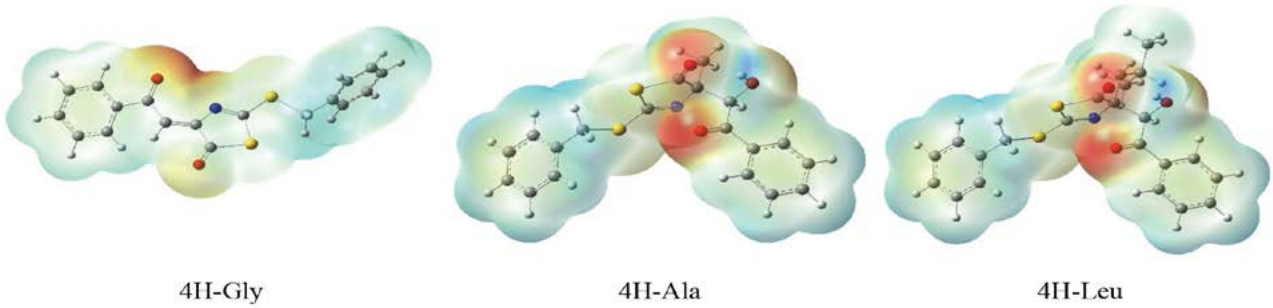


**Figure 3.** Electrostatic potential map for 4H-Gly, 4H-Ala and 4H-Leu products.

tive regions of the electrostatic potential are localized mainly around the hydrogen atoms attached to the phenyl rings.

To obtain more information about the sites which are more probable to be involved in nucleophilic attack, the maximum potential electrostatic values were determined and some of them are listed in Table 6. Data in Table 6 indicate that in the case of 4H-Gly the C18 is more nucleophilic than the C11. C15 is more nucleophilic than C13 indicating that the Michael addition occurred on C15 and then the structure of the main regioisomer could be predicted. In the case of the 4H-Ala and 4H-Leu products, the C15 and C11 are determined as the most nucleophilic sites.

**Table 6.** Maximum electrostatic potentials in kcal/mol for some selected atoms of 4H-Gly, 4H-Ala and 4H-Leu products.

| 4H-Gly | | 4H-Ala | | 4H-Leu | |
|---|---|---|---|---|---|
| **Atom** | ***Vs*(Max)** | **Atom** | ***Vs*(Max)** | **Atom** | ***Vs*(Max)** |
| C11 | 9.30 | C11 | 6.48 | C11 | 7.62 |
| C13 | 5.55 | C13 | 6.74 | C13 | 5.88 |
| C15 | 15.67 | C15 | 8.06 | C15 | 5.48 |
| C16 | 6.30 | C19 | 0.00 | C19 | 0.00 |
| C18 | 15.67 | C40 | 0.00 | C39 | 0.00 |

## 5. Conclusion

In conclusion, we have shown that the dithiocarbamates prepared with natural amino acids can be simply used in the Erlenmeyer–Plöchl reaction. We also have presented an efficient procedure for the synthesis of 15 novel derivatives of the thiazolactone skeleton via Erlenmeyer–Plöchl reaction without using any catalyst and harsh conditions in good to high yields. Thereafter, quantum chemical calculations were used to deeply investigate the structural characteristics and charge distribution analysis of the newly prepared products. $^1$H NMR spectra of the products were computed and compared with the experimental ones. The results revealed that there is a good agreement between calculated and experimentally obtained $^1$H NMR chemical shifts.

### Conflict of interest

The authors declare no conflict of interest.

### Acknowledgements

Support of this work from the Research Council of the University of Guilan is gratefully appreciated.

## 6. References

1. E. Erlenmeyer, *Ann.,* **1893**, 275, 1–8. **DOI:**10.1002/jlac.18932750103
2. D. Benedlt, V. Daniel, *J. Med. Chem.,* **1994**, *37*, 710–712. **DOI:**10.1021/jm00031a023
3. E. R. Pereira, M. Sancelme, A. Voldoire, M. Prudhomme, *Bioorganic Med. Chem. Lett.,* **1997**, *7*, 2503–2506. **DOI:**10.1016/S0960-894X(97)10007-5
4. A. El-Mekabaty, *I. J. Org. Chem.*, **2013**, *2*, 40–66.
5. M. A. F. El-Kaschef, F. M. E. Abdel-Megeid, S. M. A. Yassin, *Ann. Chem.,* **1974**, *1,* 37–43. **DOI:**10.1002/jlac.197419740106
6. E. Erlenmeyer, *Ber.,* **1889**, *22*, 792–795. **DOI:**10.1002/cber.188902201174
7. J. L. Diaz, B. Villacampa, F. Lopez-Calahorra, D. Velasco, *Tetrahedron Lett.*, **2002**, *43,* 4333–4337. **DOI:**10.1016/S0040-4039(02)00806-7
8. G. Koczan, G. Csik, A. Csampai, E. Balog, S. Bosze, P. Sohar, F. Hudecz, *Tetrahedron*, **2001**, *57*, 4589–4598. **DOI:**10.1016/S0040-4020(01)00332-5
9. S. Fozooni, A. M. Tikdari, H. Hamidian, H. Khabazzadeh, *Arkivoc,* **2008**, *xiv*, 115–123. **DOI:**10.3998/ark.5550190.0009.e13
10. N. Illy, E. Mongkhoun, *Polym. Chem.*, **2022**, *13*, 4592–4614. **DOI:**10.1039/D2PY00731B
11. C. Gündoğdu, D. Topkaya, G. Öztürk, S. Alp, Y. Ergün, *J. Heterocycl. Chem.*, **2010**, *47*, 1450–1453. **DOI:**10.1002/jhet.499
12. D. S. A. Haneen, W. S. I. Abou-Elmagd, A. S. A. Youssef, *Synth. Commun.*, **2021**, *51*, 215–233. **DOI:**10.1080/00397911.2020.1825746
13. M. Bergmann, F. Stern, *Ann.* **1926**, *448,* 20–31. **DOI:**10.1002/jlac.19264480103
14. A. Ziyaei Halimehjani, P. Aghabozorg Naneva, Y. Lotfi Nosod, B. Khalili, *NSMSI (In Persian)*, **2016**, *35*, 43–55.
15. B. Eftekhari-Sis, M. Zirak, A. Akbari, *Chem. Rev.*, **2013**, *113*, 2958–3043. **DOI:**10.1021/cr300176g
16. B. Khalili, P. Jajarmi, B. Eftekhari-Sis, M. M. Hashemi, *J. Org. Chem.*, **2008**, *73,* 2090–2095. **DOI:**10.1021/jo702385n
17. B. Khalili, T. Tondro, M. M. Hashemi, *Tetrahedron*, **2009**, *65,* 6882–6887. **DOI:**10.1016/j.tet.2009.06.082
18. M. Rimaz, H. Mousavi, L. Nikpey, B. Khalili, *Res. Chem. Intermed.,* **2017**, *43*, 3925–3937. **DOI:**10.1007/s11164-016-2848-5
19. M. Rimaz, P. Pourhossein, B. Khalili, *Turk. J. Chem.*, **2015**, *39*, 244–254. **DOI:**10.3906/kim-1408-32
20. M. Rimaz, H. Rabiei, B. Khalili, R. H. Prager, *Aust. J. Chem.*, **2014,** *67*, 283–288.
21. M. Rimaz, F. Aali, B. Khalili, R. H. Prager, *Aust. J. Chem.*, **2016**, *70*, 660–668. **DOI:**10.1071/CH16364
22. M. Rimaz, H. Mousavi, B. Khalili, F. Aali, *J. Chin. Chem. Soc.*, **2018**, *65*, 1389–1397. **DOI:**10.1002/jccs.201700470
23. M. Rimaz, B. Khalili, G. Khatyal, H. Mousavi, F. Aali, *Aust. J. Chem.*, **2017**, *70*, 1274–1284. **DOI:**10.1071/CH17146
24. M. Rimaz, H. Mousavi, L. Ozzar, B. Khalili, *Res. Chem. Intermed.*, **2019**, *45*, 2673–2694. **DOI:**10.1007/s11164-019-03757-9
25. M. Rimaz, J. Khalafy, H. Mousavi, S. Bohlooli, B. Khalili, *J. Heterocycl. Chem.,* **2017,** *54*, 3174–3186. **DOI:**10.1002/jhet.2932
26. N. O. Mahmoodi, B. Khalili, O. Rezaeianzade, A. Ghavidast,

*Res. Chem. Intermed.,* **2016**, *42*, 6531–6542. **DOI:**10.1007/s11164-016-2478-y
27. B. Khalili, F. Sadeghzadeh Darabi, B. Eftekhari-Sis, M. Rimaz, *Monatsh. Chem.,* **2013**, *144*, 1569–1572. **DOI:**10.1007/s00706-013-1038-z
28. S. J. Ahmadi, S. Sadjadi, M. Hosseinpour, *Ultrason Sonochem.,* **2013**, *20*, 408–412. **DOI:**10.1016/j.ultsonch.2012.07.008
29. H. A. Riley, A. R. Gray, *Org. Synth.*, **1935**, *Coll. 15*, 67–69. **DOI:**10.15227/orgsyn.015.0067
30. M. J. Frisch, G. W. Trucks, H. B. Schlegel, G. E. Scuseria, M. A. Robb, J. R. Cheeseman, G. Scalmani, V. Barone, B. Mennucci, G. A. Petersson, H. Nakatsuji, M. Caricato, X. Li, H. P. Hratchian, A. F. Izmaylov, J. Bloino, G. Zheng, J. L. Sonnenberg, M. Hada, M. Ehara, K. Toyota, R. Fukuda, J. Hasegawa, M. Ishida, T. Nakajima, Y. Honda, O. Kitao, H. Nakai, T. Vreven, J. A. Montgomery, Jr., J. E. Peralta, F. Ogliaro, M. Bearpark, J. J. Heyd, E. Brothers, K. N. Kudin, V. N. Staroverov, R. Kobayashi, J. Normand, K. Raghavachari, A. Rendell, J. C. Burant, S. S. Iyengar, J. Tomasi, M. Cossi, N. Rega, J. M. Millam, M. Klene, J. E. Knox, J. B. Cross, V. Bakken, C. Adamo, J. Jaramillo, R. Gomperts, R. E. Stratmann, O. Yazyev, A. J. Austin, R. Cammi, C. Pomelli, J. W. Ochterski, R. L. Martin, K. Morokuma, V. G. Zakrzewski, G. A. Voth, P. Salvador, J. J. Dannenberg, S. Dapprich, A. D. Daniels, Ö. Farkas, J. B. Foresman, J. V. Ortiz, J. Cioslowski, D. J. Fox, *Gaussian 09, Revision A.11.4*, **2009**, Gaussian Inc., Wallingford CT.
31. A. D. Becke, *J. Chem. Phys.,* **1993**, *98*, 5648–5652. **DOI:**10.1063/1.464913
32. C. T. Lee, W. T. Yang, R. G. Parr, *Phys. Rev. B* **1988**, *37*, 785–789. **DOI:**10.1103/PhysRevB.37.785
33. M. J. Frisch, J. A. Pople, J. S. Binkley, *J. Chem. Phys.,* **1984,** *80*, 3265–3269. **DOI:**10.1063/1.447079
34. P. C. Chen, Y. C. Chieh, J. C. Wu, *J. Mol. Struct.,* **2005**, *715*, 183–189. **DOI:**10.1016/j.theochem.2004.10.012
35. E. K. U. Gross, W. Kohn, *Adv. Quantum Chem.*, **1990**, *21*, 255–291.
36. A. Streitwieser, *Molecular Orbital Theory for Organic Chemists*, **1961,** Wiley, New York. **DOI:**10.1149/1.2425396
37. A. Eşme, S. Güneşdoğdu Sağdınç, *Spectrochim. Acta A,* **2018**, *188*, 443–455. **DOI:**10.1016/j.saa.2017.07.034
38. J. K. M. Sanders, B. K. Hunter, *Modern NMR Spectroscopy. A Guide for Chemists, Magnetic Resonance in Chemistry*, Oxford University Press, Oxford, **1987**, *25*, 1092. **DOI:**10.1002/mrc.1260251217
39. J. R. Cheeseman, G. W. Trucks, T. A. Keith, and M. J. Frisch, *J. Chem. Phys.*, **1996**, *104*, 5497–5509. **DOI:**10.1063/1.471789
40. J. X. Mao, *JPR*, **2014**, *2*, 15–18.
41. R. S. Mulliken, *J. Chem. Phys.,* **1955,** *23*, 1833–1840. **DOI:**10.1063/1.1740588
42. R. S. Mulliken, *J. Chem. Phys.,* **1955**, *23*, 1841–1846. **DOI:**10.1063/1.1740589
43. R. S. Mulliken, *J. Chem. Phys.,* **1955**, *23*, 2338–2342. **DOI:**10.1063/1.1741876
44. A. E. Reed, R. B. Weinstock, F. Weinhold, *J. Chem. Phys.,* **1985**, *83*, 735–746. **DOI:**10.1063/1.449486
45. P. Politzer, J. Murray, *Theor. Chem. Acc.*, 2002, *108*, 134–142. **DOI:**10.1007/s00214-002-0363-9
46. P. Politzer, J. S. Murray, *Theoretical Biochemistry and Molecular Biophysics: A Comprehensive Survey,* **1991**, Adenine Press, New York.

## Povzetek

V okviru te raziskave smo s pomočjo Erlenmeyer–Plöchlove reakcije sintetizirali 15 derivatov s tiazolaktonskim skeletom. Kot prekurzorje ditiokarbamata smo uporabili aminokisline glicin, alanin in levcin tako, da smo jih reagirali z ogljikovim disulfidom in benzil kloridom. Dobljene benzil ditiokarbamate smo v prisotnosti acetanhidrida pretvorili v ustrezne tiazolaktone ter jih v nadaljevanju kondenzirali z arilglioksali kot viri karbonilne skupine. Produkte smo karakterizirali s spektroskopskimi metodami IR, $^{1}$H NMR in $^{13}$C NMR. V nadaljevanju smo s pomočjo računskih metod pridobili dodatne informacije o produktih, vključno z njihovimi strukturnimi značilnostmi, razporeditvijo nabojev ter $^{1}$H NMR in UV-VIS spektri. Rezultati so pokazali, da se izračunane vrednosti kemijskih premikov dobro ujemajo z eksperimentalno izmerjenimi. Za vse izračune smo uporabili B3LYP DFT metodo skupaj s 6-311++G(d,p) baznim setom.